

[Home](#) [Search](#) [Collections](#) [Journals](#) [About](#) [Contact us](#) [My IOPscience](#)

## Isomers and alignments in $^{191}\text{Ir}$ and $^{192}\text{Os}$

This article has been downloaded from IOPscience. Please scroll down to see the full text article.

2012 J. Phys.: Conf. Ser. 381 012060

(<http://iopscience.iop.org/1742-6596/381/1/012060>)

View [the table of contents for this issue](#), or go to the [journal homepage](#) for more

Download details:

IP Address: 150.203.19.87

The article was downloaded on 25/09/2012 at 01:21

Please note that [terms and conditions apply](#).

## Isomers and alignments in $^{191}\text{Ir}$ and $^{192}\text{Os}$

G D Dracoulis<sup>1</sup>, G J Lane<sup>1</sup>, A P Byrne<sup>1</sup>, H Watanabe<sup>1,2</sup>,  
R O Hughes<sup>1</sup>, N Palalani<sup>1</sup>, F G Kondev<sup>3</sup>, M P Carpenter<sup>4</sup>,  
D Seweryniak<sup>4</sup>, S Zhu<sup>4</sup>, R V F Janssens<sup>4</sup>, C J Lister<sup>4</sup>, T Lauritsen<sup>4</sup>,  
P Chowdhury<sup>5</sup>, Y Shi<sup>6</sup> and F R Xu<sup>6</sup>

<sup>1</sup> Department of Nuclear Physics, R.S.P.E., Australian National University, Canberra, A.C.T. Australia 0200

<sup>2</sup> RIKEN Nishina Center, 2-1 Hirosawa, Wako, Saitama 351-0198, Japan

<sup>3</sup> Nuclear Engineering Division, Argonne National Laboratory, Argonne IL, U.S.A.

<sup>4</sup> Physics Division, Argonne National Laboratory, Argonne IL, U.S.A.

<sup>5</sup> Department of Physics, University of Massachusetts Lowell, Lowell, MA 01854, U.S.A.

<sup>6</sup> School of Physics, Peking University, Beijing 100871, China

E-mail: george.dracoulis@anu.edu.au

**Abstract.** Deep-Inelastic reactions have been used to populate high-spin states in the even-even osmium isotopes and in the iridium neighbors. New isomers have been identified in  $^{190}\text{Os}$ ,  $^{192}\text{Os}$ ,  $^{194}\text{Os}$ ,  $^{191}\text{Ir}$  and  $^{193}\text{Ir}$ . These include a 2 ns  $12^+$  state at 2865 keV and a 295 ns,  $20^+$  state at 4580 keV in  $^{192}\text{Os}$ . Although a number of multi-quasiparticle states arising from prolate and triaxial deformations are expected in these nuclei, the main structures in  $^{192}\text{Os}$  can be interpreted as a two-stage alignment of  $i_{13/2}$  neutrons at oblate deformation, in close analogy with similar structures in the isotones  $^{194}\text{Pt}$  and  $^{196}\text{Hg}$ . The isomers are attributed to low-energy  $E2$  transitions at the point of the alignment gains. The isomer observed in  $^{191}\text{Ir}$  is long-lived ( $\tau_m \sim 8$  s) and probably arises from coupling of the  $h_{11/2}$  proton to the  $10^- \nu 9/2^- [505] 11/2^+ [615]$  prolate configuration that gives rise to long-lived isomers in  $^{190}\text{Os}$  and  $^{192}\text{Os}$ , although potential-energy-surface calculations indicate that the resultant three-quasiparticle state will be triaxial.

### 1. Introduction

The nuclear structure of the even-even isotopes of osmium,  $^{186}\text{Os}$ ,  $^{188}\text{Os}$ ,  $^{190}\text{Os}$  and  $^{192}\text{Os}$  is of considerable interest since they fall in the transitional region where static and dynamic effects due to the triaxial degree of freedom are expected to be important. Their description is challenging for theoretical models. The seminal Coulomb excitation studies of Wu *et al.* [1, 2] that exploited model-independent sum rules, concluded that the stable osmium nuclei are indeed  $\gamma$ -soft, but prolate deformed. While  $^{190}\text{Os}$  and  $^{192}\text{Os}$ , for example, have average asymmetry angles close to  $20^\circ$  and  $24^\circ$  respectively, these are well localized.

Despite the interest, the proximity of nuclei in this region to the stability line has meant that high-spin spectroscopic information has been limited. However, with the development of deep-inelastic and fragmentation reactions for spectroscopic studies, both stable and neutron-rich isotopes are becoming accessible. For example, results on the ground state bands for  $^{188}\text{Os}$  and  $^{190}\text{Os}$  have been reported [3], as well as for the neutron-rich isotope  $^{194}\text{Os}$  [4] and some yrast states in  $^{198}\text{Os}$  have been identified with fragmentation [5].

Recent theoretical studies include extensive mean field calculations that describe ground- and excited-state shape evolution [6, 7, 8, 9, 10] across the range of neutron-rich Hf, W, Os and Pt nuclei. In a more specific prediction, Walker and Xu [11] have proposed that a rotation-aligned oblate structure would compete with the (largely) prolate structures in the isotones  $^{190}\text{W}$  and  $^{192}\text{Os}$  since the Fermi surface is close to the low- $\Omega$  orbitals within the  $i_{13/2}$  neutron shell at oblate deformation (thus maximising Coriolis effects), but near the top of the shell at prolate deformation. Both limits could give low-lying  $12^+$  states, that could also be isomers.

Isomers occur for several reasons, such as when low energy and/or high multiplicities are involved [12]. So-called  $K$ -isomers arise when the  $\gamma$ -ray multipolarity  $\lambda$  fails to match the difference in  $K$  between the initial and final states, (where  $K$  is the projection of the total angular momentum on the nuclear deformation axis) the shortfall  $\nu = \Delta K - \lambda$  being termed the forbiddenness. The resultant hindrance ( $F$ ) is given by the ratio of the partial  $\gamma$ -ray lifetime compared to the Weiskopff estimate, so that  $F = \tau_\gamma/\tau_W$ . In well-deformed nuclei, the hindrance is found to scale so that the reduced hindrance  $f_\nu = F^{1/\nu}$  is approximately a constant of magnitude  $\sim 100$ . Experimental reduced hindrances  $f_\nu$  can be taken as indicators of the “goodness” of  $K$  although it should be remembered that rotational effects will broaden the  $K$  distributions in a well-defined (calculable) fashion, random state mixing may be present ( see [13] for examples of both), and fluctuations in shape could undermine the purity of  $K$  since the projection axis is no longer fixed.

As should be clear from the above, the presence or absence of isomers, or whether their lifetimes are long or short, is not necessarily evidence of dilution of the  $K$ -quantum number. The qualitative expectation that  $K$ -isomerism will diminish as the perimeter of the well-deformed region is crossed, needs to be quantified in terms of transition strengths. In  $^{190}\text{Os}$  and  $^{192}\text{Os}$ , for example, despite their  $\gamma$ -softness, isomers with very long lifetimes are known and attributed to the  $K^\pi = 10^- \nu 11/2^+$  [615],  $9/2^-$  [505] (prolate-deformed) configuration. The long lifetimes (14 min. in  $^{190}\text{Os}$  and 9 s in  $^{192}\text{Os}$ ) arise because of the low-energy, high-multipolarity decays ( $M2$  and  $E3$ ) and also because of  $K$ -hindrance, even though the reduced hindrances are all anomalously low ( $\leq 10$ ).

## 2. Experimental Details

The present measurements to study nuclei in this region used 6.0 MeV per nucleon  $^{136}\text{Xe}$  beams provided by the ATLAS facility at Argonne National Laboratory. Nanosecond pulses, separated by 825 ns, were incident on enriched  $^{186}\text{W}$  and  $^{192}\text{Os}$  targets. Gamma-rays were detected with Gammasphere, with 100 detectors in operation. Triple coincidences were required and the main data analysis was carried out with  $\gamma$ - $\gamma$ - $\gamma$  cubes with various time-difference conditions, and also with time constraints relative to the pulsed beam to select different out-of-beam regimes.

Another set of measurements was carried out using a macroscopically chopped beam with various (beam on)/(beam off) conditions. In these, out-of-beam dual coincidence events were recorded in reference to a precision clock and  $\gamma$ - $\gamma$  matrices as a function of the time were constructed in contiguous time regions, allowing long lifetimes to be isolated by gating on cascades of interest. Scans were made with different conditions, progressing in steps of ten, from initial values in the sub-millisecond region up the region of a few seconds.

The results on a range of even-even osmium and odd- $A$  iridium isotopes will be reported in due course, the main focus here being on preliminary results for  $^{191}\text{Ir}$  and  $^{192}\text{Os}$ . Results for the neutron-rich isotopes  $^{188}\text{W}$  and  $^{190}\text{W}$  from the same measurements were published recently [14].

## 3. Iridium isotopes and $^{191}\text{Ir}$

The lightest odd- $A$  iridium isotope identified was  $^{187}\text{Ir}$ , corresponding to the removal of five neutrons from the  $^{192}\text{Os}$  target, and the heaviest was  $^{195}\text{Ir}$ , from the addition of three neutrons. The main new results are for  $^{191}\text{Ir}$  and  $^{193}\text{Ir}$ . In  $^{191}\text{Ir}$ , feeding from a long-lived, but unidentified

isomer, into states in the rotational band based on the  $h_{11/2}$  proton (the  $11/2^-$  [505] Nilsson orbital) had been reported in early studies using the  $^{192}\text{Os}(d,3n)^{191}\text{Ir}$  reaction [15]. The  $h_{11/2}$  band is also known in  $^{193}\text{Ir}$  [16], but no isomers had been reported. We have also obtained coincidence information on delayed transitions in  $^{195}\text{Ir}$ , previously identified from fragmentation studies [17]. A large number of other transitions depopulating isomers in iridium nuclei, most probably in the odd-odd isotopes, have been identified, but as yet not assigned to specific nuclei, largely because of the absence of information on low-lying high-spin bands in those nuclei.

Selected spectra obtained with double gates on delayed transitions in  $^{191}\text{Ir}$  are given in Fig. 1. The lower panel (figure 1(b)) shows the delayed transitions feeding into the  $19/2^-$  state of the

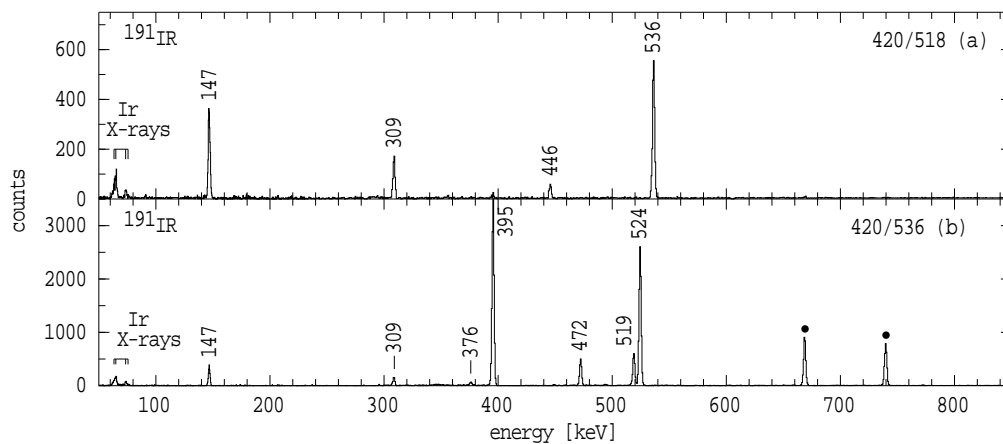


**Figure 1.** Out-of-beam  $\gamma$ -ray spectra in  $^{191}\text{Ir}$  with double  $\gamma$ -ray coincidence gates as indicated. Known contaminants are indicated by the symbol ( $\bullet$ ).

$11/2^-$  band, the main path being through the cascade of 524-keV and 395-keV transitions directly above. This was the path identified previously, with a delayed component attributed to an unobserved transition from a long-lived isomer with  $E^* \leq 2123$ -keV and  $T_{1/2} = 5.5(7)$  s, (corresponding to a meanlife of  $7.9(10)$  s), feeding a state at 2047 keV.

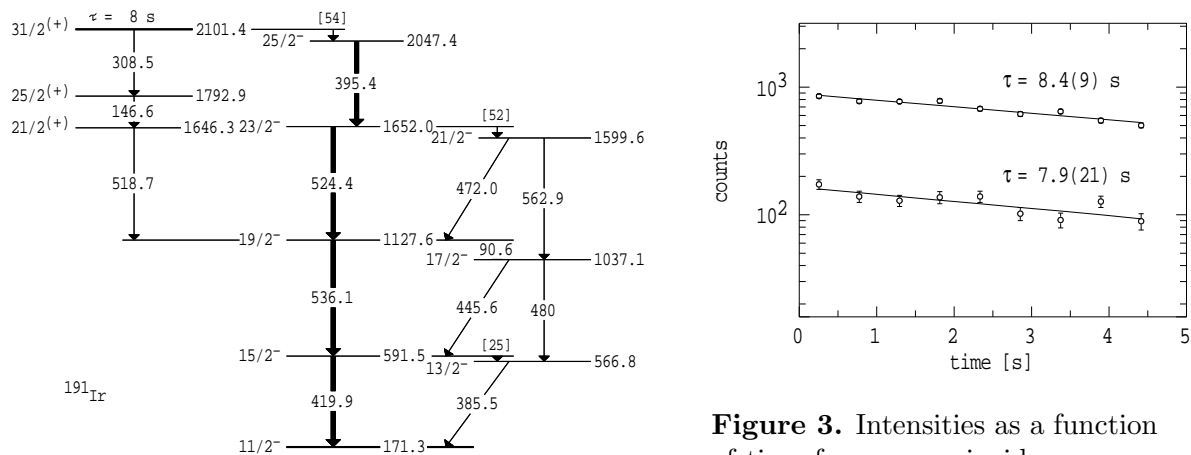


**Figure 2.** Partial level scheme for  $^{191}\text{Ir}$ , showing the main decays from the isomer and the  $h_{11/2}$  band.

**Figure 3.** Intensities as a function of time from  $\gamma$ - $\gamma$  coincidence spectra selecting the two delayed paths in  $^{191}\text{Ir}$  together with fits that return the meanlives indicated.

The partial level scheme deduced from the present work is given in Fig. 2, with spins and parities based on a consideration of total conversion coefficients deduced from delayed intensity balances and  $\gamma$ - $\gamma$  angular correlations. The 395 keV transition is a mixed dipole, and probably therefore of  $E2/M1$  character. This leads to a  $J^\pi = 25/2^-$  assignment for the 2047 keV state. Although it could be a candidate for the  $25/2^-$  member of the unfavoured sequence of the  $11/2^- [505]$  band, we do not observe the expected  $E2$  branch to the  $21/2^-$  member. As well, the angular correlation obtained by gating on stretched quadrupoles lower in the scheme is of opposite sign to those of the 472-keV and 446-keV transitions (see Fig. 2). While the mixing ratio is not consistent with the 395-keV transition being a band member, there is an alignment in this region, and therefore a change in structure that needs to be considered.

Our results confirm the main transitions, but an additional delayed path is evident from the coincidence spectra given in figure 1. The cascade of 308.5, 146.6 and 518.7 keV transitions feeds the  $19/2^-$ , 1128 keV level, implying a state at 2101.4 keV, 54 keV above the 2047.4-keV,  $25/2^-$  state. Our contention is that the 2101.4 keV state is the isomer, with an unobserved 54-keV transition to the 2047.4 keV state. This is consistent with the observation in the earlier work of prompt feeding to the 2047 keV state [15], and the fact that we observe the same lifetime for both paths, evidence for which is shown in figure 3.

The 308.5 keV  $M3$  transition strength is  $1.52(15) \times 10^{-3}$  W.u., while the implied 54 keV  $E3$  branch has a strength of  $1.62(14) \times 10^{-2}$  W.u., both reasonable values, although a full evaluation would need characterisation of the final state configurations. The present calculations of the expected intrinsic states that allow for shape variations with configuration constraints [18, 19], predict a  $31/2^+$  state from the  $\nu 11/2^+ [615], 9/2^- [505] \otimes \pi 11/2^- [505]$  configuration at 2210 keV, close to the observed energy of the isomer. Unlike the core,  $10^-$  two-neutron component however, the equilibrium deformation has a  $\gamma$ -asymmetry of about  $27^\circ$ . In fact, the calculations predict a number of other intrinsic states in this energy region including a  $31/2^-$  state from the  $\nu 11/2^+ [615], 9/2^+ [624] \otimes \pi 11/2^- [505]$  configuration (calculated to lie at at 2086 keV).

#### 4. The Nuclide $^{192}\text{Os}$

The main delayed transitions in  $^{192}\text{Os}$  are apparent in the spectrum in figure 4 obtained by summing selected double gates on the yrast transitions that are not fed by the long-lived  $10^-$  isomer. A partial level scheme is given in figure 5. Transitions above the 295 ns isomer placed

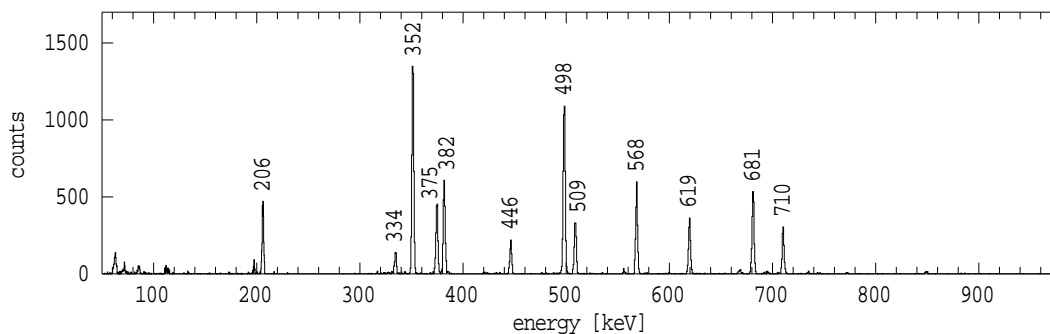


**Figure 4.**  $\gamma$ -ray spectrum produced by summing double  $\gamma$ -ray coincidence gates in  $^{192}\text{Os}$  in the 100-700 ns out-of-beam time region.

at 4580 keV with an 85-keV decay, preceding the 382, 568, 681-keV cascade, were identified using time-correlated gates on the lower transitions. Other key features of the scheme include the 2 ns,  $12^+$  state at 2865 keV which has several decay paths, including  $E2$  transitions to two  $10^+$  states, but a dominant decay via an  $E1$  transition of 498 keV to the  $11^-$  state of the  $10^-$

band. This, and other branches, have allowed the identification of the band based on the  $10^-$  isomer, normally inaccessible because of its very long lifetime.

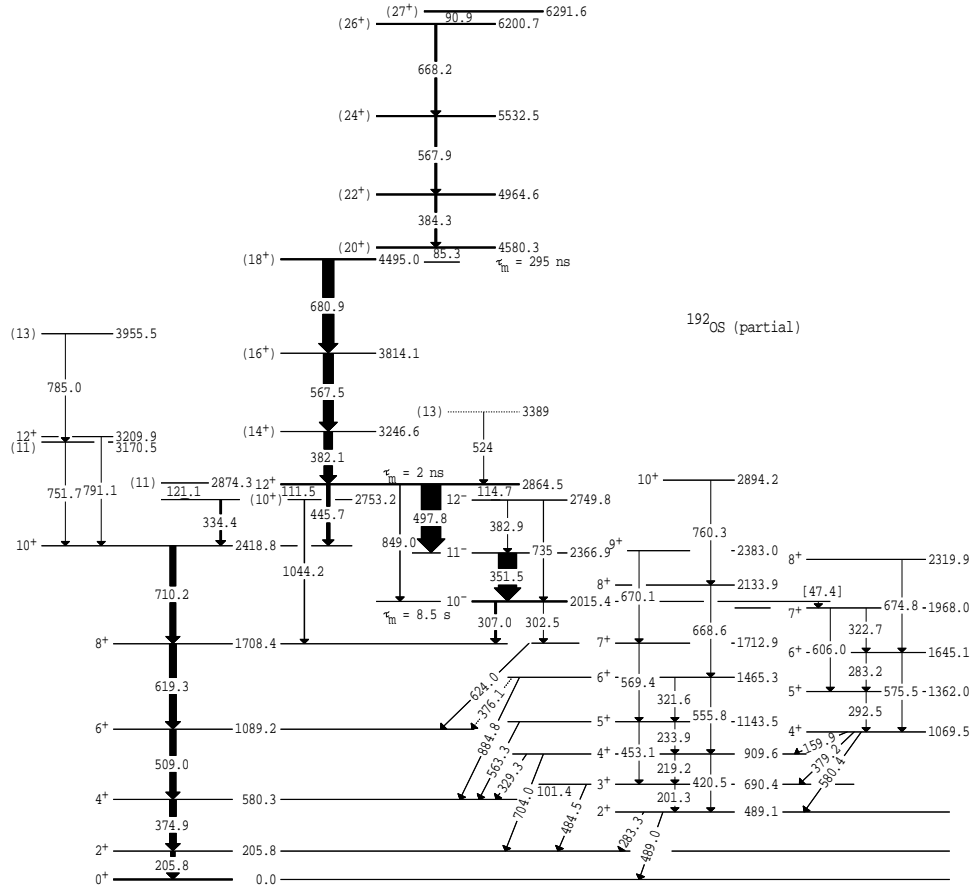
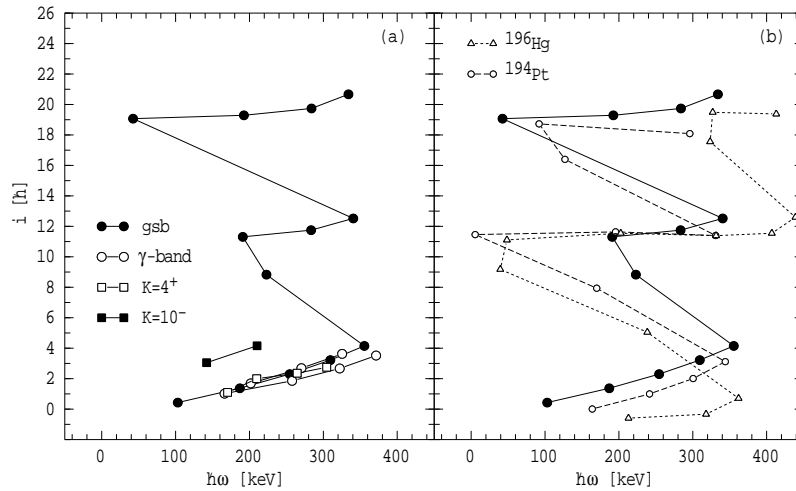


Figure 5. Partial level scheme for  $^{192}\text{Os}$ .

The net alignments of the band structures are illustrated in figure 6(a). For the discussion, these have been evaluated using a reference which is appropriate for an oblate deformation. Because of this, the low-frequency trajectories of the ground-band,  $\gamma$ -band and  $K = 4^+$  band, while essentially the same, have an artificial upward slope. The  $10^-$  band shows about  $3\hbar$  more alignment, consistent with the presence of the  $11/2^+[615]$ ,  $i_{13/2}$  neutron orbital in its configuration and there are two sharp increments, beginning near the  $12^+$  and  $20^+$  states, corresponding to alignment gains of  $\sim 12\hbar$  and  $\sim 8\hbar$  respectively. The main sequence is compared with that of the isotones  $^{194}\text{Pt}$  and  $^{196}\text{Hg}$  [21]. Most of the yrast sequence for  $^{194}\text{Pt}$  proposed by Jones *et al.* [20] and interpreted as being of oblate collectivity, has been confirmed in the present measurements, but some modifications were necessary and are reflected in figure 6(b).

The comparison between these cases seems compelling: Very similar alignment gains are observed, consistent with the *AB* and *CD* alignments expected for the  $i_{13/2}$  neutron shell when the Fermi level is close to the low- $\Omega$  orbitals, as is the case for oblate deformation. This is the accepted interpretation for  $^{196}\text{Hg}$  [21]. The first alignment is just that predicted for the  $^{192}\text{Os}$  case in Ref. [11]. Similar  $12^+$  isomers occur in both  $^{194}\text{Pt}$  and  $^{196}\text{Hg}$ , with comparable transition strengths. In the present case, the 111.5 keV  $E2$  transition from the  $12^+$  state to the  $10_2^+$  state, presumably the lower-spin member of the *s*-band, has a strength of 9.7(26) W.u., while the competing 445.7 keV  $E2$  to ground state band is much weaker, at  $4.4(9)\times 10^{-2}$  W.u.. The  $20^+ \rightarrow 18^+$ , 85.3 keV transition is 0.99(4) W.u.. Two

of these can be seen as essentially collective transitions, modified by the change in intrinsic structure caused by the alignment gain. Although various intrinsic states are predicted by the



**Figure 6.** (a) Net alignments for bands in  $^{192}\text{Os}$ . (b) comparison of net alignment curves for the isotones  $^{192}\text{Os}$ ,  $^{194}\text{Pt}$  and  $^{196}\text{Hg}$ , with a common reference.

calculations in the same energy region, including a prolate four-quasineutron  $20^+$  level from the  $11/2^+[615], 13/2^+[606], 7/2^- [503], 9/2^- [505]$  configuration, the current conclusion would be that the observed  $20^+$ , 295 ns and  $12^+$ , 2 ns isomers in  $^{192}\text{Os}$  are products of alignment gains within the set of  $i_{13/2}$  neutron orbitals at oblate deformation.

### Acknowledgments

This work was supported by the Australian Research Council Discovery Programme and the U.S. Department of Energy, Office of Nuclear Physics, under Contract No. DE-AC02-06CH11357 and Grant No. DE-FG02-94ER40848.

### References

- [1] C Y Wu *et al.*, Nucl. Phys. A **607**, 178 (1996).
- [2] C Y Wu and D Cline, Phys. Rev. C **54**, 2356 (1996).
- [3] S Mohammadi, *et al.* Int. J. Mod. Phys. E **15**, 1797 (2006).
- [4] C Wheldon *et al.* Phys.Rev. C **63**, 011304 (2001).
- [5] Zs Podolyak *et al.* Phys.Rev. C **79**, 031305 (2009).
- [6] L M Robledo, R Rodriguez-Guzman, P Sarriguren J. Phys. G **36**, 115104 (2009).
- [7] P Sarriguren, R Rodriguez-Guzman, L M Robledo Phys. Rev. C **77**, 064322 (2008).
- [8] R Fossion, D Bonatsos, G A Lalazissis Phys. Rev. C **73**, 044310 (2006).
- [9] P D Stevenson *et al.* Phys. Rev. C **72**, 047303 (2005).
- [10] K Nomura *et al.* Phys. Rev. **83**, 054303 (2011).
- [11] P M Walker and F R Xu, Phys. Lett. B **635**, 286 (2006).
- [12] P M Walker and G D Dracoulis Nature **399**, 35 (1999).
- [13] G D Dracoulis *et al.* Phys.Rev.Lett. **97**, 122501 (2006).
- [14] G J Lane *et al.* Phys. Rev. C **82**, 051304(R) (2010).
- [15] J Lukasiak, R Kaczarowski, J Jastrzebski, S Andre, J Treherne, Nucl.Phys. **A313**, 191 (1979).
- [16] Y D Fang *et al.* Phys.Rev. C **83**, 054323 (2011).
- [17] S J Steer *et al.*, Int. J. Mod. Phys. E **18**, 1002 (2009).
- [18] F R Xu, P M Walker, J A Sheikh and R Wyss, Phys. Lett. B **435**, 257 (1998).
- [19] F R Xu, Chin. Phys. Lett. **18**, 750 (2001).
- [20] G A Jones *et al.*, Acta Physica Pannonica B **36**, 1323 (2005).
- [21] D Mehta *et al.*, Z. Phys. A **339**, 317 (1991).